Cancer Research

Sialic Acid Blockade Suppresses Tumor Growth by Enhancing T-cell–Mediated Tumor Immunity

Christian Büll[1], Thomas J. Boltje[2], Natasja Balneger[1], Sarah M. Weischer[1], Melissa Wassink[1], Jasper J. van Gemst[3], Victor R. Bloemendal[2], Louis Boon[4], Johan van der Vlag[3], Torben Heise[2], Martijn H. den Brok[1,5], and Gosse J. Adema[1]

Abstract

Sialic acid sugars on the surface of cancer cells have emerged as potent immune modulators that contribute to the immunosuppressive microenvironment and tumor immune evasion. However, the mechanisms by which these sugars modulate antitumor immunity as well as therapeutic strategies directed against them are limited. Here we report that intratumoral injections with a sialic acid mimetic $Ac_5 3F_{ax}Neu5Ac$ block tumor sialic acid expression *in vivo* and suppress tumor growth in multiple tumor models. Sialic acid blockade had a major impact on the immune cell composition of the tumor, enhancing tumor-infiltrating natural killer cell and $CD8^+$ T-cell numbers while reducing regulatory T-cell and myeloid regulatory cell numbers. Sialic acid blockade enhanced cytotoxic $CD8^+$ T-cell–mediated killing of tumor cells in part by facilitating antigen-specific T-cell–tumor cell clustering. Sialic acid blockade also synergized with adoptive transfer of tumor-specific $CD8^+$ T cells *in vivo* and enhanced CpG immune adjuvant therapy by increasing dendritic cell activation and subsequent $CD8^+$ T-cell responses. Collectively, these data emphasize the crucial role of sialic acids in tumor immune evasion and provide proof of concept that sialic acid blockade creates an immune-permissive tumor microenvironment for $CD8^+$ T-cell–mediated tumor immunity, either as single treatment or in combination with other immune-based intervention strategies.

Significance: Sialic acid sugars function as important modulators of the immunosuppressive tumor microenvironment that limit potent antitumor immunity.

Graphical Abstract: http://cancerres.aacrjournals.org/content/canres/78/13/3574/F1.large.jpg. *Cancer Res; 78(13); 3574–88. ©2018 AACR.*

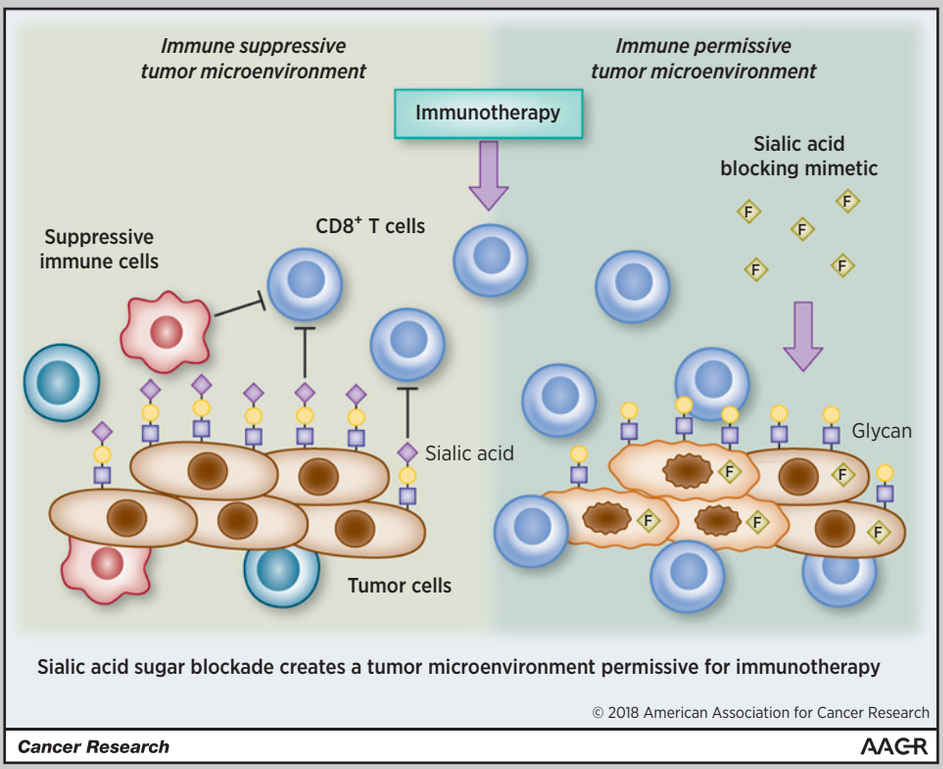

Sialic acid sugar blockade creates a tumor microenvironment permissive for immunotherapy

Cancer Research AACR

[1]Radiotherapy & OncoImmunology Laboratory, Department of Radiation Oncology, Radboud Institute for Molecular Life Sciences, Radboud University Medical Center, Nijmegen, the Netherlands. [2]Cluster for Molecular Chemistry, Institute for Molecules and Materials, Radboud University Nijmegen, Nijmegen, the Netherlands. [3]Department of Nephrology, Radboud Institute for Molecular Life Sciences, Radboud University Medical Center, Nijmegen, the Netherlands. [4]Bioceros, Utrecht, the Netherlands. [5]Department of Anesthesiology, Pain and Palliative Medicine, Radboud University Medical Center, Nijmegen, the Netherlands.

Note: Supplementary data for this article are available at Cancer Research Online (http://cancerres.aacrjournals.org/).

T.J. Boltje and N. Balneger contributed equally to this article.

Current address for S.M. Weischer: Department of Cell Biology, Radboud Institute for Molecular Life Sciences, Radboud University Medical Center, Geert Grooteplein 26-28, Nijmegen 6525 GA, the Netherlands.

Corresponding Author: Gosse J. Adema, Radiotherapy & OncoImmunology Laboratory, Department of Radiation Oncology, Radboud Institute for Molecular Life Sciences, Radboud University Medical Center, Geert Grooteplein Zuid 32, Nijmegen 6525 GA, the Netherlands. Phone/Fax: 310-2-4361-4023; E-mail: Gosse.Adema@radboudumc.nl

doi: 10.1158/0008-5472.CAN-17-3376

Introduction

Altered glycosylation is a hallmark of virtually all cancer cells from different origins, and several aspects of tumor growth and progression are mediated by tumor-associated glycans (1, 2). One of the most remarkable changes in cancer glycosylation is the aberrant expression of sialic acid–carrying glycans (sialoglycans) (3). Sialic acids are a family of negatively charged, nine-carbon sugar molecules that often terminate the glycans of cell surface glycoproteins and glycolipids. Human cancer cells cover their membrane with a dense layer of sialoglycans and also express unique sialoglycans on their surface (e.g., SLe^a/^{x}, STn, GM2/3, GD2/3, or SSEA-4; refs. 4–6). Tumor sialoglycans facilitate cancer cell migration and metastasis formation and moreover tumor sialoglycans emerge as potent immune modulators that promote tumor immune evasion (3, 7–10). Already in the 1960s, it was proposed that the dense layer of sialic acids surrounding tumor cells protects them from recognition and eradication by the immune system, and even clinical trials were performed using irradiated cancer cells treated with bacterial sialidase as vaccine in patients with cancer. At that time, however, contradicting data and the lack of effective glycotools to provide further mechanistic insight dampened the enthusiasm of the scientific community (11–13). Recent developments in glycoengineering have revitalized research on the potential role of sialic acids in the antitumor immune response. These studies in human and animal models have shown that tumor sialic acids negatively influence immune cell function by interacting with the immune-inhibitory sialic acid–binding immunoglobulin-like lectin (Siglec) family (14–19). Tumor sialic acid–Siglec interactions, therefore, are believed to modulate immune cell function and hinder antitumor immunity (7, 8, 10, 20–22).

Approaches to interfere with sialoglycan expression in cancer *in vivo* are, however, still limited and barely tested in preclinical tumor models. So far, mainly bacterial sialidases or tumor cells with genetically silenced sialic acid expression were used to study the effects of tumor sialic acids (9, 18, 23). While these approaches are useful to study some aspects of tumor sialylation, they are difficult to apply in a therapeutic setting to interfere with sialic acid expression in established tumors. Pharmacologic inhibition of sialic acid expression in tumors *in vivo*, however, has not been feasible so far. Our group has reported that a fluorinated sialic acid mimetic, $Ac_53F_{ax}Neu5Ac$, originally reported by Rillahan and colleagues, potently blocked sialic acid expression in various human and mouse cancer cell lines (24–26). $Ac_53F_{ax}Neu5Ac$ blocks sialic expression directly by the inhibition of sialyltransferases, the enzymes that incorporate sialic acids into glycans and indirectly by stopping the production of natural sialic acids in the cell (24, 27). Previously, we found that blocking sialylation with $Ac_53F_{ax}Neu5Ac$ impaired cancer cell adhesion and migration *in vitro* and prevented metastasis formation *in vivo* (26, 28). Here we explored the potential of $Ac_53F_{ax}Neu5Ac$ to block sialic acid expression in the tumor mass and investigated the consequences thereof on the tumor microenvironment and antitumor immunity.

Our data demonstrate that intratumoral injections of $Ac_53F_{ax}Neu5Ac$ blocked sialylation in tumors *in vivo* and suppressed tumor growth in different murine tumor models. Mechanistic studies revealed dominant effects on the tumor microenvironment and dependence on CD8$^+$ T cells. Sialic acid blockade potentiated cellular immunotherapy as well as CpG immunotherapy through enhanced maturation of dendritic cells in the tumor microenvironment favoring the induction of CD8$^+$ T cells. These data emphasize the important role of sialic acids in tumor immune evasion and identify $Ac_53F_{ax}Neu5Ac$ as potential prototype therapeutic molecule for the use in cancer immunotherapy.

Materials and Methods

Mice

Female C57BL/6JRccHsd WT mice (Harlan Laboratories) 8 to 10 weeks old at the beginning of the experiments were housed in the local Central Animal Laboratory. OT-I mice that produce CD8$^+$ T cells with a transgenic T-cell receptor specific for the chicken ovalbumin (OVA) epitope SIINFEKL ($OVA_{257-264}$) presented on MHC I H-2k^b and the congenic marker CD45.1$^+$ were bred in the Central Animal Laboratory. Animals were housed under specific pathogen-free conditions and *ad libitum* access to food and water. All animal experiments were authorized by the local animal ethics committee and carried out in accordance with their guidelines.

Reagents and antibodies

$Ac_53F_{ax}Neu5Ac$ and $Ac_5Neu5Ac$ were synthesized as described previously (24–26). Carbo-free blocking solution, biotinylated lectins MALII, SNA-I, and PNA were purchased from Vector Laboratories Inc., streptavidin-PE from BD Pharmingen and eFluor 780 viability dye and anti-CD11b-biotin (M1/70) from eBioscience, Inc. CD8 (2.43), CD4 (GK1.5), NK1.1 (PK136) and Gr-1 (RB6.8C5) depleting mAbs were produced by culturing hybridomas in Iscove's modified Dulbecco's medium with 1% FBS. Clodronate liposomes were purchased from Liposoma B.V., $OVA_{257-264}$ (SIINFEKL) was purchased from AnaSpec Inc., and CpG ODN 1826 from InvivoGen. *Clostridium perfringens* sialidase, β-galactosidase, and DAPI were purchased from Sigma-Aldrich. CFSE, PBSE, and AF488-conjugated streptavidin were obtained from Thermo Fisher Scientific and anti-CD16/CD32 (2.42G), anti-CD45.2-biotin (104), and anti-CD161/NK1.1-PE (PK136) from BD Pharmingen. Anti-CD8α-AF700 (53-6.7) was purchased from EXBIO and anti-CD4-PerCP (RM4-5), anti-CD11c-APC (N418), anti-CD11b-AF700 (M1/70), anti-CD45R/B220-PerCp (RA3-6B2), anti-H-2K^b/H-2D^b-PE (28-8-6), and anti-CD8α -biotin (53-6.7) from BioLegend. Anti-CD25-APC (PC61.5), anti-FoxP3-PE-Cy7 (FJK-16s), anti-Mult-1-PE (5D10) and anti-CD274/PD-L1-PE (MIH5) were obtained from eBioscience and anti-Rae-1-APC (FAB17582A) from R&D Systems. Anti-biotin-Cy3 was obtained from Jackson ImmunoResearch.

Cell culture and titration of $Ac_53F_{ax}Neu5Ac$

B16-F10^{WT} melanoma cells were obtained from and authenticated by ATCC (CRL-6475) and cultured in minimum essential medium (MEM; Gibco) containing 5% FBS (Greiner Bio-one), 1% MEM nonessential amino acids (Gibco), 0.15% sodium bicarbonate (Gibco), 1 mmol/L sodium pyruvate (Gibco), 1.5% MEM vitamins (Gibco), 1% antibiotic–antimycotic solution (PAA). B16-F10^{OVA} cells (clone MO5) were kindly provided by Dr. Kenneth Rock and cultured in B16-F10^{WT} medium supplemented with 200 μg/mL geneticin (Gibco) and Hygromycin B (Merck; ref. 29). No full authentication of the B16-F10^{OVA} cells was carried out by the authors, but the expression of OVA, TRP-2, TRP-2, MHC I, and other molecules was validated. The 9464D neuroblastoma cell line

(kindly provided by R. Orentas, Department of Pediatrics, Medical College of Wisconsin, WI) was authenticated last by the authors in 2013 by qPCR analysis of neuroblastoma-specific genes. 9464D cells were cultured in DMEM Glutamax (Gibco) with 10% FBS, 1% nonessential amino acids, 20 μmol/L 2-mercaptoethanol (Sigma-Aldrich) and 1% antibiotic–antimycotic solution (30, 31). All cell lines were initially grown and multiple aliquots were cryopreserved. The cells were used within 3 months after resuscitation and regularly tested for *Mycoplasma* using a *Mycoplasma* Detection Kit (Lonza). To compare the effect of Ac_53F_{ax}Neu5Ac on sialic acid expression between B16-F10^{WT} and B16-F10^{OVA} cells, both cell lines were incubated for 3 days with 100 μmol/L Ac_53F_{ax}Neu5Ac. To determine the effective dose of Ac_53F_{ax}-Neu5Ac in 9464D cells, they were incubated for 3 days with 0–500 μmol/L sialic acid mimetic. Sialylation was quantified by flow cytometry using lectins as described below. All cells were incubated in a humidified CO_2 incubator at 37°C.

In vivo tumor experiments

Following reconstitution from liquid nitrogen, tumor cell lines were cultured in T75 flasks (Corning), passaged twice, and grown to 60%–70 % confluency. Cells were collected in 1× PBS at a concentration of 0.5×10^6 cells/mL (B16-F10^{WT}), 1×10^6 cells/mL (B16-F10^{OVA}), or 1×10^7 cells/mL (9464D) and 100 μL of the cell suspension was injected subcutaneously into the right flank of the mice under isoflurane anesthesia. Tumor size was examined every 2–3 days and tumor volumes were calculated with the formula $[(A \times B^2) \times 0.4]$, in which A is the largest and B is the shortest tumor dimension. Mice were sacrificed when the tumor volume exceeded 1,800 mm^3. Ac_53F_{ax}Neu5Ac and Ac_5Neu5Ac were dissolved in 1× PBS, and on day 10 when a palpable tumor mass was formed 50 μL of 1× PBS containing 10, 20, or 30 mg/kg sialic acid mimetic were injected into the tumor mass thrice per week. Optional, CpG was injected into the tumor mass on day 14 and 21 postinoculation. Naïve mice were injected subcutaneously three times per week with sialic acid mimetic for two weeks. PBS only injections were used as control. For rechallenge experiments in the B16-F10^{OVA} model, 3×10^4 B16-F10^{OVA} cells were injected subcutaneously into the left femur of mice with remission after the initial tumor challenge or naïve, age-matched control mice and tumor growth was monitored in time. For the depletion of $CD4^+$, $CD8^+$, $NK1.1^+$, or Gr-1^+ cells *in vivo* 300 μg depleting mAbs or isotype control antibodies were injected intraperitoneally either two days before tumor inoculation or on day 6, 8, and 20 after tumor inoculation, respectively. Clodronate liposomes (1 mg/mouse) were injected intraperitoneally on day 8 postinoculation and from day 10 onwards. Mice received 0.25 mg injections twice per week until the end of the experiment to maintain depletion.

Preparation of single-cell suspensions

Mice were sacrificed by cervical dislocation and the tumor, spleen, draining, and non-draining lymph nodes (superficial inguinal) were isolated. Tumors and spleens were mashed through a 100-μm nylon cell strainer and collected in 1× PBS and red blood cells were lysed by incubating the suspension for 1 minute in ice-cold ACK lysis buffer (150 mmol/L NH_4Cl, 10 mmol/L $KHCO_3$, and 0.1 mmol/L Na_2-EDTA, pH 7.2). Lymph nodes were comminuted between glass slides and single cells were harvested in 1× PBS.

Intra/extracellular cell staining and flow cytometry analysis

For extracellular staining with biotinylated lectins, the cells were washed with 1× carbo-free blocking solution and incubated for 45 minutes at 4°C with MALII (5 μg/mL), SNA-I (1 μg/mL), or PNA (5 μg/mL) in 1× carbo-free blocking solution containing 1 mmol/L $CaCl^{2+}$ and 1 mmol/L $MgCl^{2+}$. Next, cells were washed with 1× carbo-free blocking solution, incubated for 20 minutes at 4°C with streptavidin–PE conjugate, washed again, and resuspended in PBA (1× PBS, 1 % BSA, and 0.02 % sodium azide) for flow cytometry analysis. For extracellular antibody staining, cells were first incubated 10 minutes at 4°C with PBA containing Fc receptor blocking antibody (2.42G), then washed with PBA and incubated for 20 minutes at 4°C with fluorescent antibodies. After extensive washing, the cells were resuspended in PBA for flow cytometry analysis or further used for intracellular staining. For intracellular stainings, a cell fixation and permeabilization kit (BD Biosciences) was used following the manufacturer's instructions. Briefly, cells were incubated for 20 minutes with 1× fix/perm solution at 4°C and washed with perm/wash buffer. Next, cells were incubated overnight with antibody in perm/wash buffer at 4°C, washed with perm/wash buffer, and resuspended in PBA for flow cytometry analysis. Cells were measured using a CyAn ADP flow cytometer (Beckman Coulter) and data were analyzed using FlowJo software (Tree Star Inc.).

Urine and blood collection and determination of albuminuria and serum urea

Naïve mice were subcutaneously injected three times a week for two weeks with PBS, 10, 20, or 30 mg/kg Ac_53F_{ax}Neu5Ac. At several time points, urine of the mice was collected and pooled per time point and treatment group and blood was collected via the tail vein into MiniCollect tubes (Greiner Bio-one). To obtain serum, the tubes were centrifuged for 10 minutes, 12,000 rpm, at room temperature. Albumin concentrations were measured by radial immunodiffusion (Mancini). Urinary creatinine and serum urea levels were determined as described previously (32).

IHC

To assess the effect of sialic acid blockade on the tumor microenvironment, B16-F10^{WT} tumors injected for two weeks with PBS or 10 mg/kg Ac_53F_{ax}Neu5Ac were isolated on day 24 postinoculation and snap frozen in liquid nitrogen. To investigate the effects of Ac_53F_{ax}Neu5Ac injections on the kidneys, naïve mice received subcutaneous injections with PBS, 10, 20, or 30 mg/kg Ac_53F_{ax}Neu5Ac three times per week for two weeks. Two or four weeks after starting the treatment, kidneys were collected and snap frozen in liquid nitrogen. IHC analysis of the tumors and kidneys was performed as described previously (33). Briefly, frozen tumor sections (5 μm) and renal sections (2 μm) were fixed in ice-cold acetone for 10 minutes and incubated with the biotinylated lectins MALII, SNA-I, or PNA diluted in PBA for 45–60 minutes. For antibody stainings, the sections were blocked for 30 minutes with 2% donkey serum and incubated for 60 minutes with anti-CD8α-biotin or anti-CD11b-biotin antibodies followed by 10 minutes staining with DAPI in PBS. Biotinylated lectins and antibodies were detected with AF488-streptavidin or anti-biotin-Cy3 antibodies. Images were acquired with a Zeiss Axio Imager M1 fluorescence microscope. Fluorescence intensity was evaluated semiquantitatively from 0 (no staining) to 10 (100 % maximum intensity) on blinded sections.

In vitro CD8$^+$ OT-I activation

To obtain activated CD8$^+$ OT-I cells, single-cell suspensions prepared from OT-I spleens were cultured for 4 days in the presence of 0.75 μg/mL $OVA_{257-264}$ peptide in RPMI1640 medium (Life Technologies) supplemented with 10 % FBS (Greiner Bio-one), 2 mmol/L glutamine (Lonza), and 1× antibiotic–antimycotic solution (100 U/mL of penicillin, 100 μg/mL of streptomycin, and 0.25 μg/mL Fungizone; Life Technologies). On day 3, 5 ng/mL recombinant mouse IL2 (ImmunoTools) was added to the culture. Following activation, CD8$^+$ OT-I cells were purified using a CD8a$^+$ T Cell isolation kit according to the manufacturer's protocol (Miltenyi Biotec).

OT-I killing and clustering assay

For *in vitro* killing assays, B16-F10^{WT}, B16-F10^{OVA}, 9464D^{WT}, or 9464D^{OVA} cells were cultured for three days with PBS, 100 μmol/L Ac_5Neu5Ac, 100 μmol/L (B16-F10), or 250 μmol/L Ac_53F_{ax}Neu5Ac. Alternatively, B16-F10 cells were treated for 60 minutes at 37°C with 250 mU/mL sialidase, 1 U/mL β-galactosidase or PNA lectin was added to the culture. The cells were extensively washed with 1× PBS and 3× 10^4 cells were seeded into 96-well flat-bottom wells (Costar). Cells were allowed to adhere for two hours before purified, activated OT-I CD8$^+$ T cells were added in different effector-to-target ratios (0.1:1, 0.25:1, 0.5:1, 1:1, 2:1). After 16 hours of coculture, images were taken and numbers of live tumor cells and CD8$^+$ CD90.1$^+$ OT-I T cells were quantified using flow cytometry. Percentage killing was calculated by normalizing the number of viable tumor cells in the cocultures to control cultures without effector T cells. To determine cluster formation between tumor cells and T cells, B16-F10^{WT} or B16-F10^{OVA} cells treated with control or 100 μmol/L Ac_53F_{ax}Neu5Ac for 3 days were labeled with 3 μmol/L PBSE and activated CD8$^+$ OT-I cells were labeled with 0.5 μmol/L CFSE following the manufacturer's instructions. B16-F10 cells and OT-I cells were incubated together in a 1:2 ratio in medium for 2 hours at 37°C rotating, fixed with PFA and the number of PBSE$^+$/CFSE$^+$ clusters was determined by flow cytometry.

Adoptive OT-I cell transfer

For adoptive transfer experiments, 1 × 10^7 purified OT-I cells were injected intraperitoneally on day 15 following inoculation. Tumor growth was monitored or tumors were isolated two days after adoptive transfer to assess OT-I CD8$^+$ T-cell infiltration and activation marker expression by flow cytometry. For the latter experiment, OT-I CD8$^+$ T cells were labeled with 3 μmol/L CFSE prior to adoptive transfer following the manufacturer's instructions.

qPCR

Expression of Siglec family members on activated OT-I CD8$^+$ T cells and total splenocytes was determined by qPCR. RNA was isolated from OT-I CD8$^+$ T cells or splenocytes using a RNA Isolation Kit (Zymo Research) following the manufacturer's instructions. RNA samples were treated in-column with DNase I and analyzed by spectrophotometry. Next, cDNA was synthesized using random hexamers and Moloney murine leukemia virus reverse transcriptase (Invitrogen). Siglec expression was determined with a CFX96 system (Bio-Rad) using SYBR Green Reaction Mix (Sigma-Aldrich). Data were calculated as relative expression to the housekeeping gene *Gapdh*. Primer sequences were derived from the Harvard Primer Bank.

Statistical analysis

Significance between two groups was calculated using a Student *t* test. Comparisons between multiple groups were made using one-way ANOVA followed by Bonferroni correction. Kaplan–Meier survival curves were analyzed with a log-rank test using Prism 5 software (GraphPad Inc.) and *P* values <0.05 were considered significant (*, $P < 0.05$; **, $P < 0.01$; ***, $P < 0.001$).

Results

Intratumoral Ac_53F_{ax}Neu5Ac injections suppress tumor growth

The sialic acid mimetic Ac_53F_{ax}Neu5Ac specifically blocks sialic acid expression in human and mouse cell lines *in vitro* without affecting cell viability or proliferation (25, 26). *In vitro* pretreatment of mouse B16-F10^{WT} melanoma cells with this sialic acid mimetic delayed their outgrowth *in vivo* following subcutaneous injection, and moreover prevented metastatic spread (26, 28). These data prompted us to investigate the effect of intratumoral administration of Ac_53F_{ax}Neu5Ac on tumor growth in different mouse tumor models. Mice bearing palpable B16-F10^{WT} tumors were injected with 10 or 30 mg/kg Ac_53F_{ax}Neu5Ac into the tumor mass three times a week for four weeks (Fig. 1A). This treatment schedule was based on our previous observation that the blocking effect of Ac_53F_{ax}Neu5Ac lasted for 2 (α2,6-linked sialic acids) to 4 days (α2,3-linked sialic acids) in B16-F10^{WT} cells after inhibitor removal (26). Injections with PBS and 10 or 30 mg/kg peracetylated nonblocking sialic acid (Ac_5Neu5Ac) were used as controls. B16-F10^{WT} tumors injected with PBS grew rapidly, resulting in a median survival time of 24 days (Fig. 1B and C). While control injections with Ac_5Neu5Ac sialic acid had no effect on tumor growth, Ac_53F_{ax}Neu5Ac injections significantly suppressed tumor growth in this stringent tumor model. In a dose-dependent manner, treatment with the sialic acid-blocking mimetic increased median survival times from 24 days to 36 (10 mg/kg) and 47 days (30 mg/kg), respectively (Fig. 1B and C; Supplementary Fig. S1).

Next, sialic acid blockade therapy with Ac_53F_{ax}Neu5Ac was tested in the related, more immunogenic ovalbumin-expressing B16-F10^{OVA} model and an unrelated 9464D neuroblastoma model. *In vitro*, B16-F10^{OVA} cells had a comparable sensitivity to Ac_53F_{ax}Neu5Ac (100 μmol/L) as B16-F10^{WT} cells, whereas a higher dose (> 250 μmol/L) was required for 9464D cells (Supplementary Fig. S2). In the 9464D model, injections of 10 mg/kg had little effect on tumor growth, whereas 20 mg/kg injections significantly increased the median survival from 40 days to 58 days (Fig. 1D). In the B16-F10^{OVA} model, 10 mg/kg Ac_53F_{ax}Neu5Ac injections strongly reduced tumor growth and resulted in complete remission in about half of the mice (Fig. 1E and F). These mice remained tumor-free for over 120 days postinoculation. Upon rechallenge of the surviving mice with B16-F10^{OVA} cells, about 60 % of the mice were protected from tumor outgrowth (Fig. 1G). The protection upon rechallenge is suggestive for a curative immune response induced by the Ac_53F_{ax}Neu5Ac injections. Furthermore, these data show that sialic acid blockade suppresses tumor growth in poorly immunogenic melanoma as well as neuroblastoma models and results in tumor regression in the more immunogenic B16-F10^{OVA} model.

In the tumor growth experiments described above, no adverse effects or weight changes were observed upon repeated intratumoral injections with the 10 mg/kg dose. In mice receiving repeated injections with 20 and 30 mg/kg Ac_53F_{ax}Neu5Ac, we

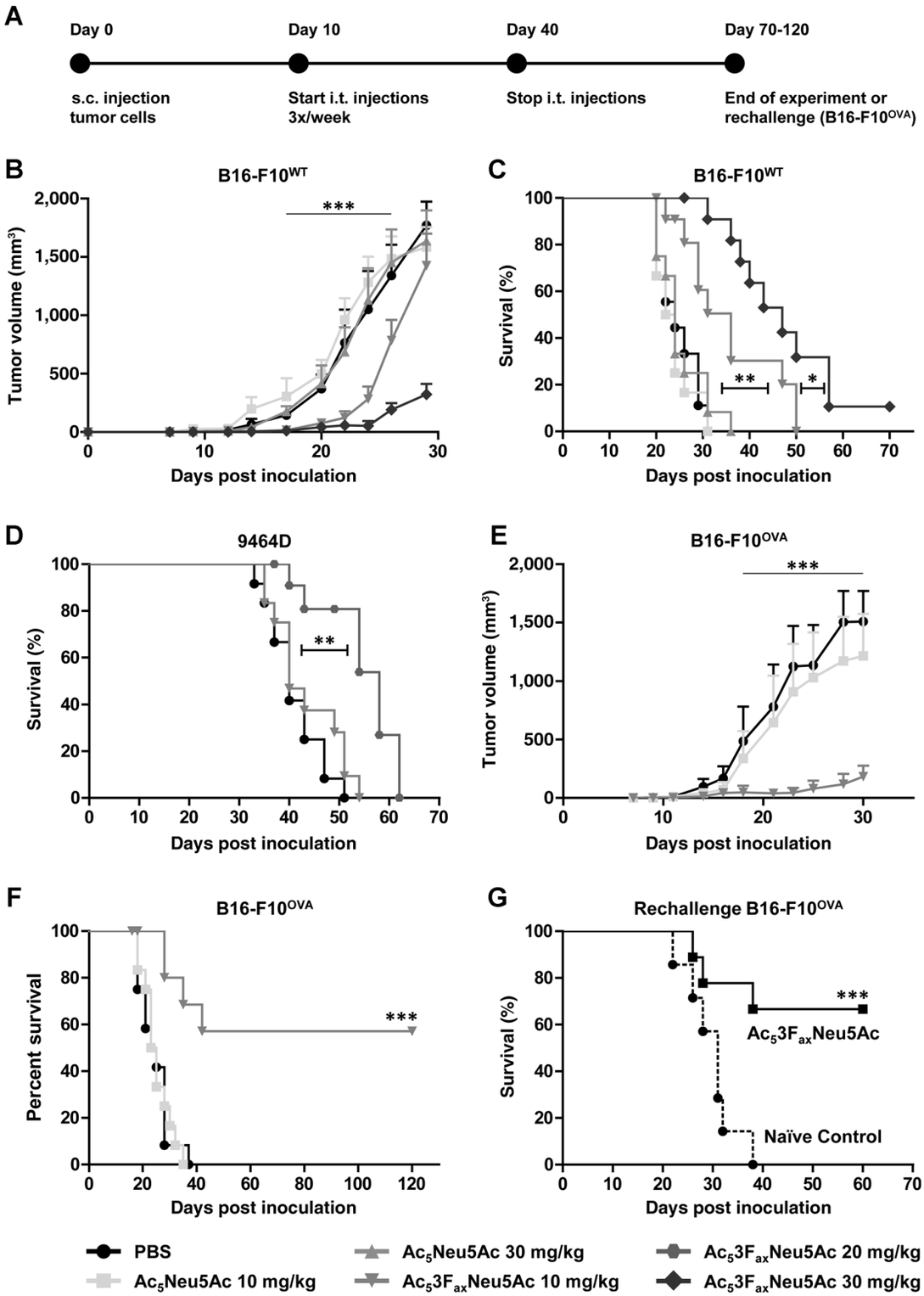

Figure 1.

Intratumoral $Ac_5 3F_{ax}Neu5Ac$ injections suppress tumor growth. **A,** Schematic representation of the experiment. **B** and **C,** Effect of intratumoral (i.t.) injections with sialic acid mimetics on B16-F10^{WT} tumor growth. B16-F10^{WT} tumor cells were inoculated subcutaneously (s.c.) and treated with PBS, 10 mg/kg or 30 mg/kg $Ac_5Neu5Ac$ or $Ac_5 3F_{ax}Neu5Ac$. Average B16-F10^{WT} tumor growth ± SEM in time (**B**) and corresponding Kaplan–Meier curves (**C**) are shown (n = 9-12). **D,** Kaplan–Meier curves showing survival of mice with 9464D neuroblastoma treated with 10 mg/kg or 20 mg/kg sialic acid mimetics (n = 12). **E** and **F,** B16-F10^{OVA}–bearing mice were injected i.t. with PBS or 10 mg/kg sialic acid mimetics (n = 9-12). Average tumor volumes ± SEM of the treatment groups in time are shown (**E**) as well as corresponding Kaplan–Meier curves (**F**). **G,** Rechallenge of mice with B16-F10^{OVA} cells after $Ac_5 3F_{ax}Neu5Ac$–induced remission of the initial primary tumor. Kaplan–Meier curves show tumor take in naïve age-matched control mice (n = 7) or rechallenged mice after $Ac_5 3F_{ax}Neu5Ac$ therapy (n = 9).

detected abdominal fluid accumulation, an increase in weight and reduced kidney function around two weeks after treatment start (Supplementary Fig. S3). No effect on kidney function was, however, observed in mice injected with 10 mg/kg Ac_53F_{ax}Neu5Ac; therefore, this dose was used for all subsequent experiments.

Ac_53F_{ax}Neu5Ac blocks sialic acid expression in the tumor mass

Next, we assessed the effect of intratumoral injections with 10 mg/kg Ac_53F_{ax}Neu5Ac or control Ac_5Neu5Ac on the sialylation of tumor cells as well as tumor-infiltrating lymphocytes. After two weeks of injections, B16-F10^{WT} tumors were isolated and analyzed by flow cytometry (Supplementary Fig. S4). Tumor cells were defined as leukocyte marker CD45.2-negative cells and immune cells as CD45.2-positive cells. Ac_53F_{ax}Neu5Ac injections reduced α2,3-sialic acid expression on tumor cells by 60% and α2,6-sialic acid expression by 50% compared with control (Fig. 2A–C). Accordingly, exposure of galactose residues was detected with PNA lectin (Fig. 2A and D). A clear reduction in sialic acid expression and exposure of galactose residues was also observed on tumor sections (Fig. 2E–G). Interestingly, in tumors injected with PBS or Ac_5Neu5Ac, more tumor cells than immune cells were present (CD45$^+$/CD45$^-$ ratio 0.32-0.43), but Ac_53F_{ax}Neu5Ac injections significantly increased the immune cell to tumor cell ratio (3.1; Fig. 2H; Supplementary Fig. S4). While Ac_53F_{ax}Neu5Ac treatment strongly reduced sialylation of tumor cells, also CD45.2$^+$ tumor-infiltrating lymphocytes showed reduced sialylation (20%; Fig. 2I–K). Noteworthy, no significant changes in the sialylation of cells in the tumor-draining lymph node, non-draining lymph nodes or spleen were detected (Supplementary Fig. S5). Altogether these data show that intratumoral injections with Ac_53F_{ax}Neu5Ac block sialic acid expression locally in the tumor mass, but not systemically. Moreover, these data indicate that tumor cells have a higher sensitivity to the sialic acid mimetics compared with infiltrating immune cells.

Sialic acid blockade alters the tumor immune cell composition

Sialic acid blockade suppressed tumor growth and even resulted in complete remission and protection from a subsequent rechallenge in the B16-F10^{OVA} model. These findings, together with the observed high tumor-infiltrating lymphocyte-to-tumor cell ratio after Ac_53F_{ax}Neu5Ac treatment, indicate that the loss of sialic acids affects tumor immunity. Therefore, we assessed the immune cell composition of B16-F10^{WT} tumors treated for two weeks with the sialic acid–blocking mimetic. Compared with PBS and Ac_5Neu5Ac-treated tumors, Ac_53F_{ax}Neu5Ac treatment increased the percentage of natural killer (NK) cells, CD8$^+$ T cells, and CD4$^+$ T cells within the viable, tumor-infiltrating lymphocyte population (Fig. 3A–G; Supplementary Fig. S6). In addition, the number of regulatory T cells was significantly reduced compared with control-injected tumors (Fig. 3D and H). Noteworthy, while the percentages of tumor-infiltrating B cells and dendritic cells remained unaltered between the treatment groups, Ac_53F_{ax}Neu5Ac injections strongly reduced the percentage of myeloid regulatory cells in the tumor (Fig. 3I–K; Supplementary Fig. S6). Similar results were obtained when performing the same experiment in the 9464D model. The immune cell composition in the (non-)draining lymph nodes and spleen remained unaltered (Supplementary Figs. S6 and S7). These results demonstrate that Ac_53F_{ax}Neu5Ac injections alter the tumor microenvironment composition, resulting in increased numbers of effector immune cells while lowering regulatory T-cell and myeloid cell numbers. Furthermore, these results indicate that sialic acid blockade converts the immunosuppressive tumor microenvironment into a more immunopermissive one.

Tumor growth suppression upon sialic acid blockade is mediated by CD8$^+$ T cells

The findings so far suggest that sialic acid blockade counteracts the immunosuppressive tumor microenvironment and influences antitumor immunity. Therefore, we investigated whether the growth-inhibitory effect of Ac_53F_{ax}Neu5Ac on established tumors was mediated by effector immune cells. B16-F10^{WT} tumor-bearing mice were depleted from NK cells, CD4$^+$ T cells, or CD8$^+$ T cells using mAbs and treated as described in Fig. 4A. Successful depletion of NK cells and T cells from the mice was confirmed (Fig. 4B–D). In line with the previous experiments, intratumoral Ac_53F_{ax}Neu5Ac injections hampered tumor growth in mice receiving isotype antibodies and increased median survival from 18.5 days to 39.5 days (Fig. 4E). Depletion of neither NK cells nor CD4$^+$ T cells had a significant effect on Ac_53F_{ax}Neu5Ac-mediated tumor growth suppression (Fig. 4E). Remarkably, depletion of CD8$^+$ T cells from mice largely abolished the antitumor effect of Ac_53F_{ax}Neu5Ac, resulting in a median survival time of only 25 days (Fig. 4F). Of note, depletion of NK cells and CD8$^+$ T cells prior to tumor cell inoculation both facilitated tumor take and abrogated the antitumor effect of Ac_53F_{ax}Neu5Ac (Supplementary Fig. S8). As expected, depletion of macrophages and myeloid cells with clodronate liposomes or anti-Gr-1 antibodies in the B16-F10^{WT} tumor model already significantly inhibited tumor growth by itself (34, 35). The finding that addition of the fluorinated sialic acid mimetic to this treatment further delayed tumor growth and significantly prolonged survival supports a role of the inhibitor beyond myeloid cells. (Supplementary Fig. S9). Altogether, these data suggest that the growth-suppressive effects of Ac_53F_{ax}Neu5Ac on established tumors is largely mediated by CD8$^+$ T cells.

Sialic acid blockade promotes tumor eradication by CD8$^+$ T cells

To further elucidate how CD8$^+$ T cells mediate the antitumor effects of Ac_53F_{ax}Neu5Ac, we assessed the cytotoxic effects of OVA-specific OT-I CD8$^+$ T cells on sialic acid–competent or deficient B16-F10^{OVA} cells *in vitro*. Sialic acid blockade strongly enhanced the eradication of B16-F10^{OVA} cells by activated OT-I CD8$^+$ T cells already at low effector-to-target ratios (Fig. 5A and B). This effect was also observed with sialidase-treated B16-F10^{OVA} cells and killing assays using 9464D^{OVA} cells as targets (Fig. 5B; Supplementary Fig. S10). B16-F10^{WT} and 9464D^{WT} cells were not sensitive to OT-I CD8$^+$ T-cell cytotoxicity, irrespective of their sialylation status. Next, we investigated whether the exposure of galactose residues upon sialic acid blockade mediated the enhanced T-cell killing. Galactose residues on B16-F10 cells were either blocked with PNA lectin or enzymatically removed. Galactosidase treatment did not alter the enhanced killing of desialylated B16-F10^{OVA} compared with control cells and incubation with PNA only slightly reduced the difference in killing (Supplementary Fig. S10). Furthermore, activated OT-I CD8$^+$ T cells expressed no immunomodulatory Siglec receptors that potentially could recognize tumor sialic acids (Supplementary Fig. S10) and treatment of B16-F10^{OVA} cells with Ac_53F_{ax}Neu5Ac had no

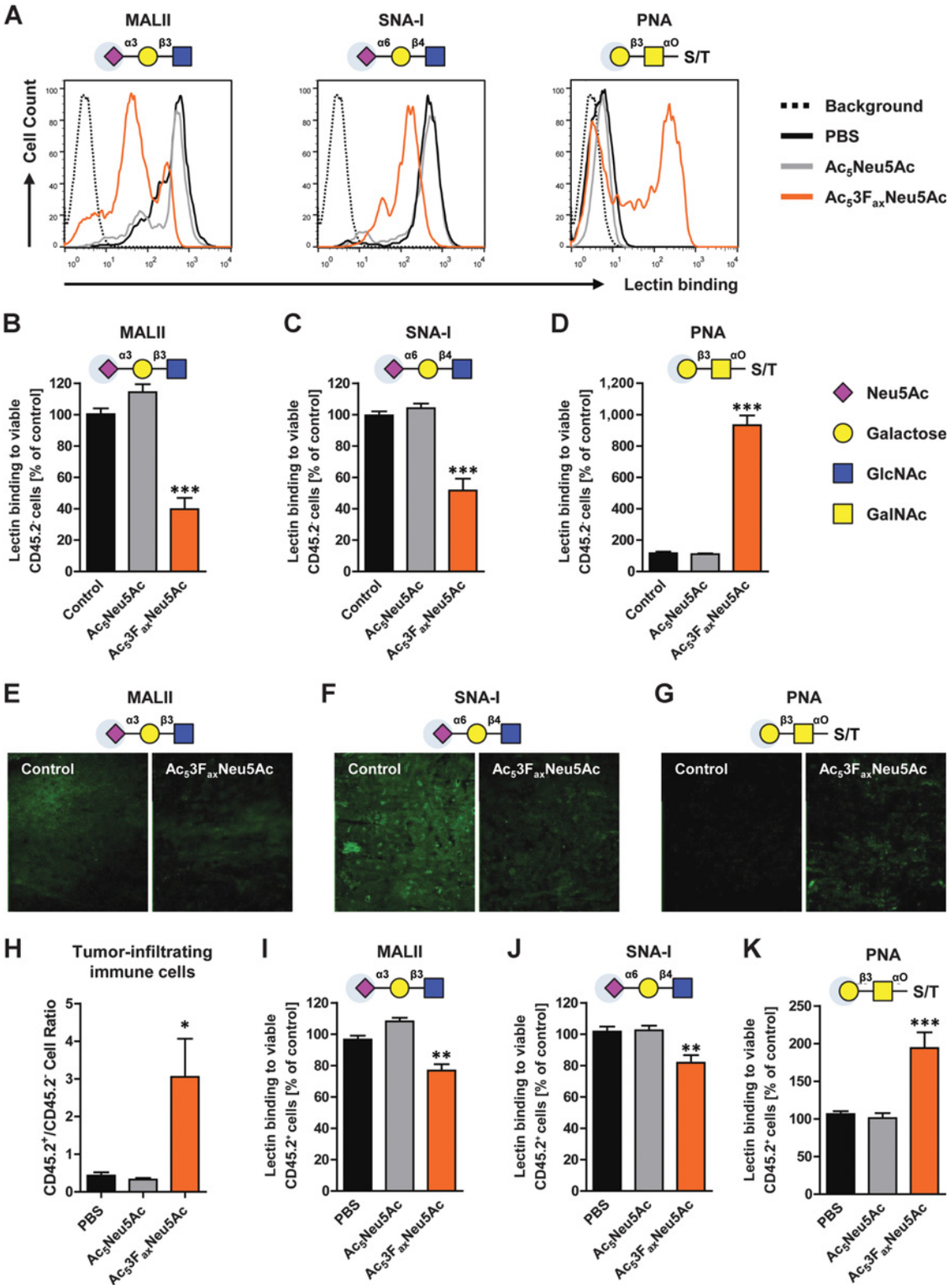

Figure 2.

$Ac_5 3F_{ax}$Neu5Ac blocks sialic acid expression and increases immune cell numbers in the tumor. **A–K,** B16-F10^{WT} tumors treated for two weeks with PBS, 10 mg/kg Ac_5Neu5Ac, or $Ac_5 3F_{ax}$Neu5Ac were isolated to determine sialylation and immune cell infiltration ($n = 6$). **A–D,** Sialylation of tumor cells (CD45.2$^-$). Representative histograms show binding of the lectins MALII, SNA-I, and PNA that recognize α2,3-linked sialic acids, α2,6-linked sialic acids, or terminal β-galactose, respectively (**A**). Bar diagrams show average binding percentages ± SEM of MALII (**B**), SNA (**C**), and PNA (**D**) to CD45.2$^-$ cells. **E–G,** Representative images show stainings of tumor sections with MALII (**E**), SNA-I (**F**), or PNA (**G**). **H,** Mean percentage ± SEM viable, tumor-infiltrating CD45.2$^+$ immune cells. **I–K,** Sialylation of immune cells (CD45.2$^+$) in the tumor. Bar diagrams show average binding percentage ± SEM of the lectins MALII (**I**), SNA-I (**J**), and PNA (**K**) to tumor-infiltrating immune cells.

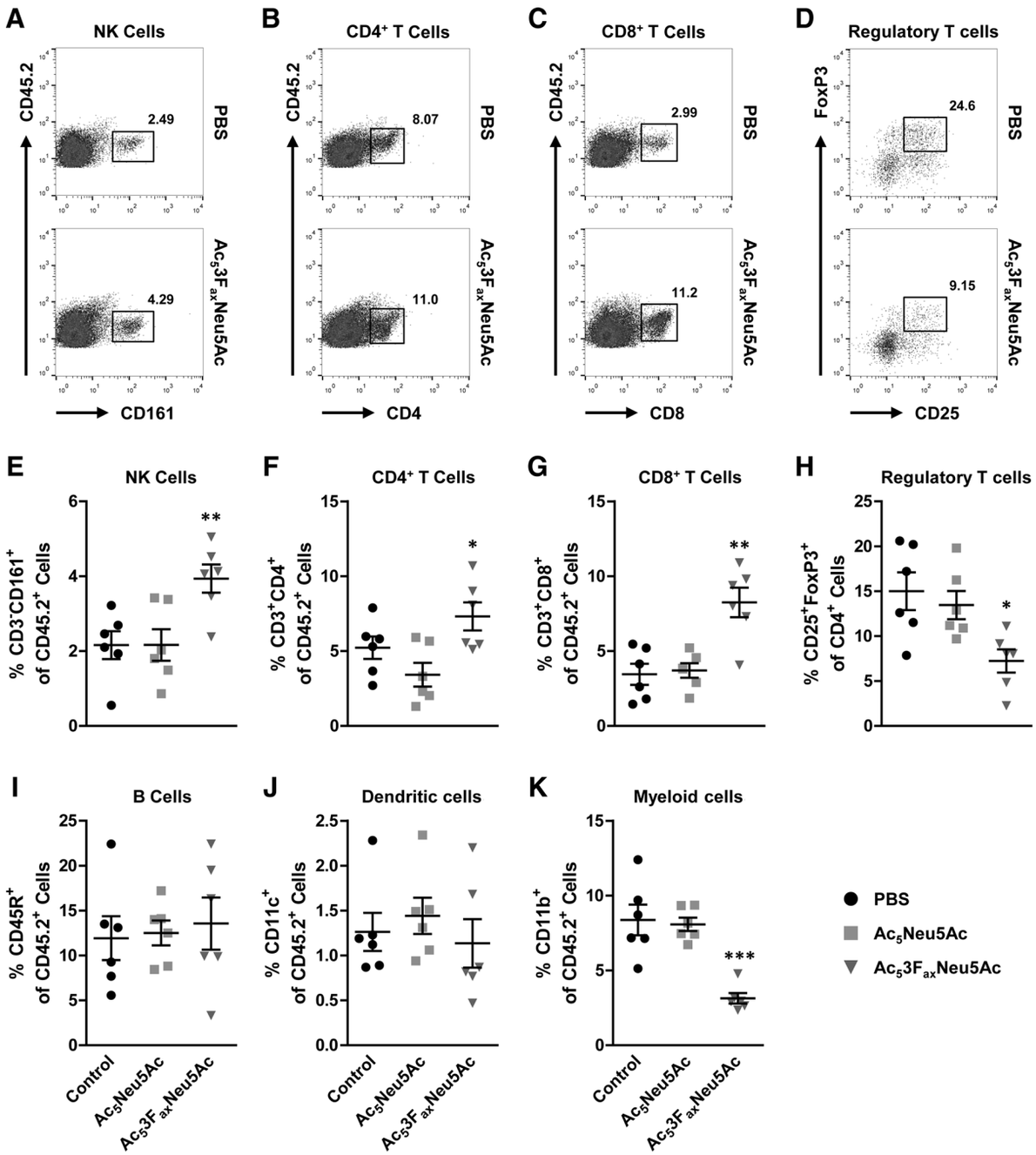

Figure 3.

Sialic acid blockade alters the immune cell composition of the tumor. **A–K,** Flow cytometry analysis of B16-F10^{WT} tumors isolated from mice treated with PBS or 10 mg/kg sialic acid mimetics for two weeks. **A–D,** Analysis of viable, CD45.2$^+$ NK cells (CD3$^-$ CD161$^+$; **A**), CD3$^+$CD4$^+$ T cells (**B**), CD3$^+$CD8$^+$ T cells (**C**), and CD4$^+$CD25^{high}FoxP3$^+$ regulatory T cells (**D**). **E–K,** Dot plots showing mean percentages ± SEM of NK cells (**E**), CD4$^+$ T cells (**F**), CD8$^+$ T cells (**G**), regulatory T cells (**H**), CD45R$^+$ B cells (**I**), CD11c$^+$ dendritic cells (**J**), and CD11b$^+$ myeloid cells (**K**) in the tumors of the different treatment groups ($n = 6$).

effect on MHC I expression or other molecules involved in effector immune cell interactions (PD-L1, Rae1, Mult-1; Supplementary Fig. S11). Moreover, the concentration of $Ac_5 3F_{ax}Neu5Ac$ used in B16-F10 cells had no effect on OT-I CD8$^+$ T-cell sialylation (Supplementary Fig. S11). Hence, the increase in OT-I CD8$^+$ T-cell killing was most likely not mediated by Siglec receptors on these cells and only to a minor extent by exposure of penultimate galactose.

Next, we investigated whether sialic acid blockade influenced the interaction of B16-F10^{OVA} cells with OT-I CD8$^+$ T cells. In tumor cell–T-cell clustering assays, B16-F10^{OVA} cells treated with $Ac_5 3F_{ax}Neu5Ac$ formed significantly more clusters (6%)

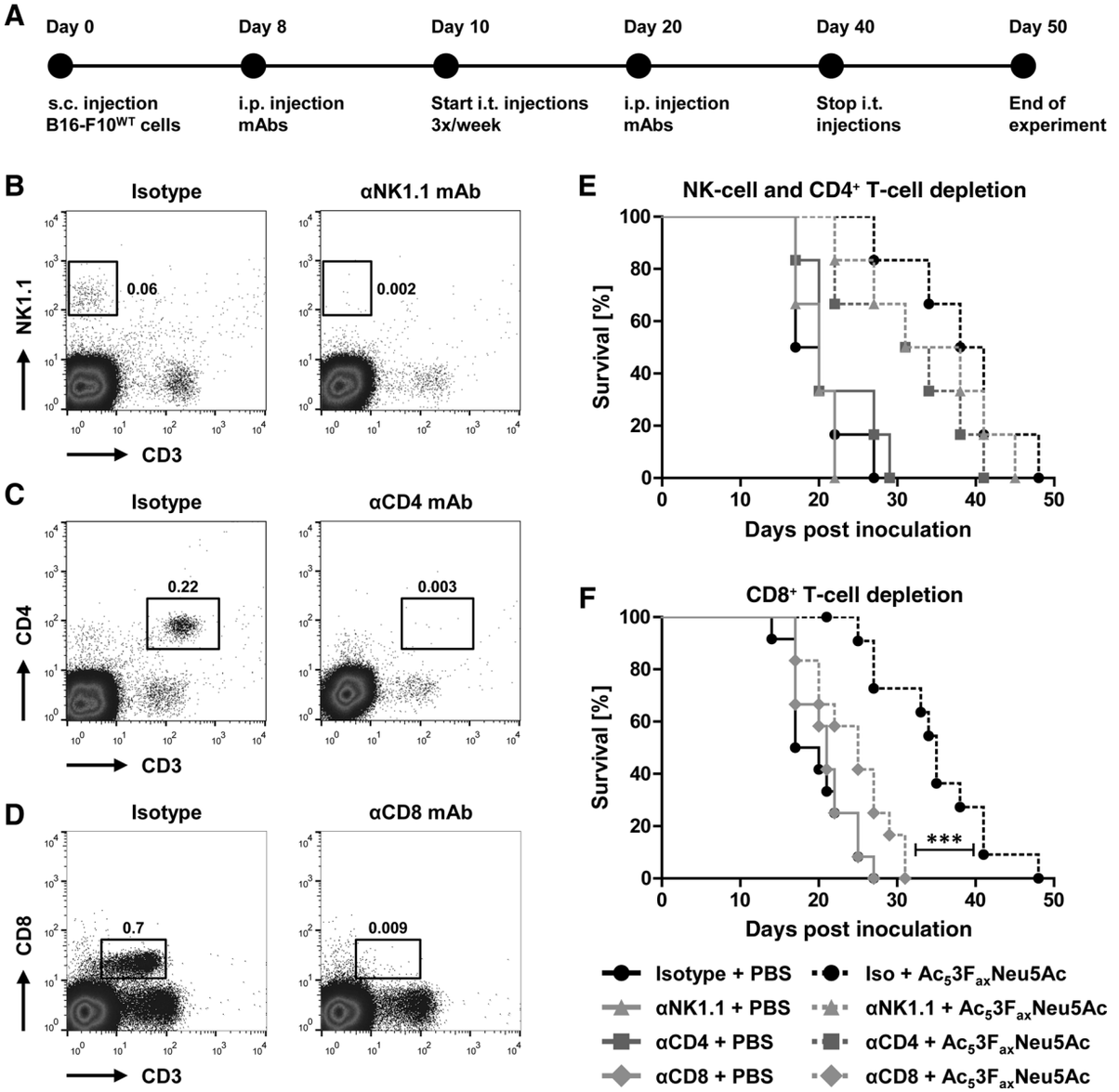

Figure 4.

Depletion of CD8$^+$ T cells abrogates the tumor-suppressive effects of $Ac_5 3F_{ax}$Neu5Ac. **A,** Schematic representation of the experiment. **B–D,** Representative dot plots showing depletion of effector immune cell subsets. NK cells (**B**), CD4$^+$ T cells (**C**), and CD8$^+$ T cells (**D**) in blood three days following isotype (left) or depleting antibody (right) injection are shown. **E,** Kaplan–Meier curves show percentage survival of B16-F10^{WT} tumor-bearing mice treated with PBS or 10 mg/kg $Ac_5 3F_{ax}$Neu5Ac in combination with isotype, CD4$^+$ T-cell, or NK-cell–depleting antibodies ($n = 6$). **F,** Kaplan–Meier curves showing percent survival of B16-F10^{WT} tumor-bearing mice depleted from CD8$^+$ T cells and treated with sialic acid mimetic or PBS ($n = 12$).

compared with control cells (3.9%; Fig. 5C and D). This effect was antigen-specific as no clear increase in cluster formation was observed in B16-F10^{WT} cells. These data indicate that sialic acid blockade increases killing of B16-F10 cells by CD8$^+$ T cells in an antigen-specific manner, possibly by facilitating cancer cell–T-cell interactions.

On the basis of these results, we tested whether sialic acid blockade enhanced OT-I CD8$^+$ T-cell–mediated tumor killing *in vivo*. Purified, activated OT-I CD8$^+$ T cells were adoptively transferred into mice bearing subcutaneous B16-F10^{OVA} tumors that were treated with PBS or $Ac_5 3F_{ax}$Neu5Ac (Fig. 6A; Supplementary Fig. S11). Sialic acid blockade significantly increased OT-I CD8$^+$ T-cell infiltration in the tumor mass (2-fold; Fig. 6B). OT-I CD8$^+$ T cells isolated from tumors treated with $Ac_5 3F_{ax}$Neu5Ac compared with control displayed a more cytotoxic phenotype with higher expression of the activation markers CD44 and CD69 and the degranulation marker CD107a (Fig. 6C–E). These results suggest that sialic acid blockade renders tumor cells vulnerable to cytotoxic CD8$^+$ T-cell killing. Accordingly, $Ac_5 3F_{ax}$Neu5Ac injections enhanced rejection of established B16-F10^{OVA} tumors

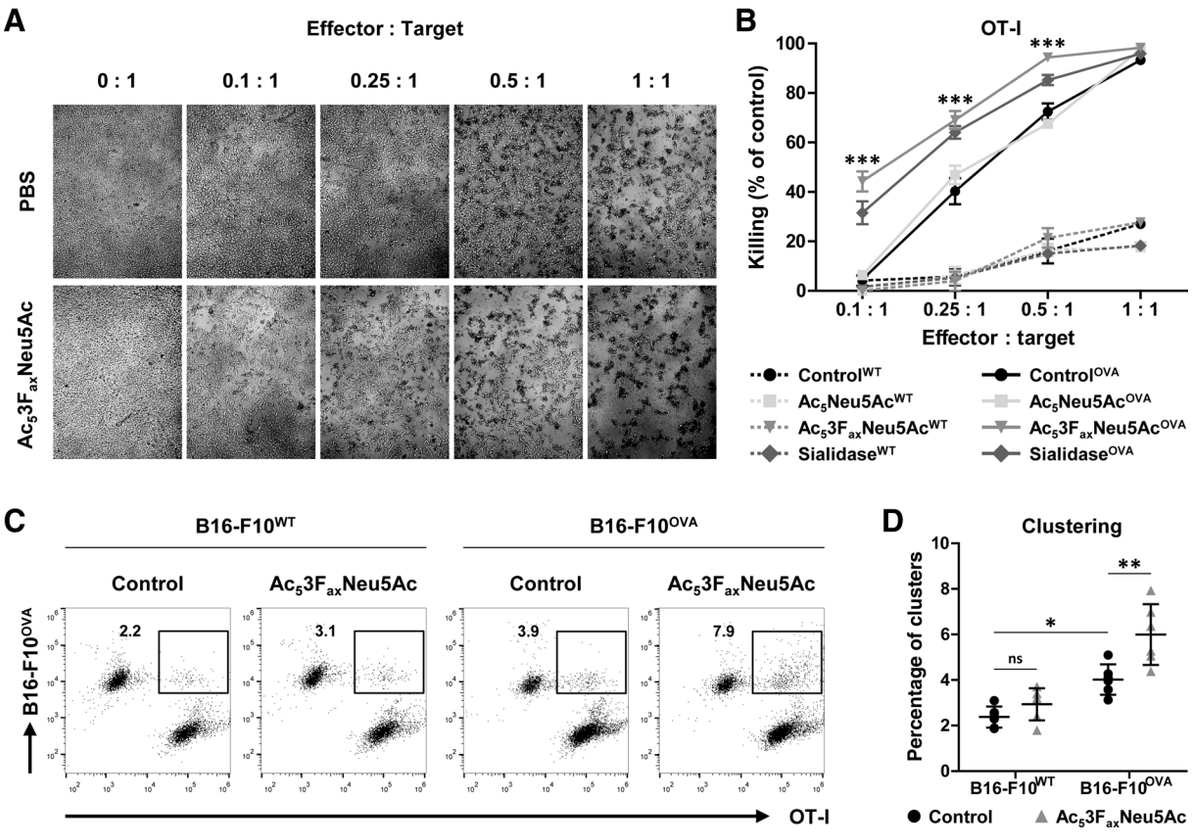

Figure 5.

Sialic acid blockade enhances tumor cell killing by cytotoxic T cells. **A** and **B,** *In vitro* killing of B16-F10^{WT} and B16-10^{OVA} target cells with blocked sialic acid expression by OVA-specific effector OT-I CD8$^+$ T cells. **A,** Representative images show lysis of B16-F10^{OVA} cells treated with PBS (top row) or $Ac_5 3F_{ax}Neu5Ac$ (bottom row). **B,** Graph shows average killing percentage ± SEM of sialic acid mimetic or sialidase-treated B16-F10^{WT} and B16-F10^{OVA} cells ($n = 6$). **C** and **D,** Effect of sialic acid blockade on B16-F10-OT-I CD8$^+$ T-cell clustering. PBSE-labeled B16-F10^{WT} or B16-F10^{OVA} cells pretreated with control or $Ac_5 3F_{ax}Neu5Ac$ were incubated with CFSE-labeled OT-I CD8$^+$ T cells. Representative plots (**C**) and dot plot (**D**) showing average number of clusters ± SEM from three independent experiments.

by adoptively transferred OT-I CD8$^+$ T cells. Without sialic acid blockade therapy, adoptive OT-I CD8$^+$ T-cell transfer enhanced median survival time from 20 days to 28 days compared with mice without T-cell transfer (Fig. 6F and G). In combination with sialic acid blockade, OT-I CD8$^+$ T-cell transfer strongly increased the median survival time of the mice and resulted in complete remission in the majority of the mice (>60%; Fig. 6F and G). Altogether, these data imply that sialic acids protect tumor cells from killing by CD8$^+$ effector T cells and that sialic acid blockade therefore facilitates T-cell-mediated tumor immunity.

Sialic acid blockade synergizes with CpG immunotherapy

On the basis of our findings that sialic acid blockade facilitates CD8$^+$ T-cell–mediated tumor immunity, we hypothesized that adjuvants able to induce CD8$^+$ T-cell responses could potentially strengthen the antitumor effect of sialic acid blockade. The Toll-like receptor 9 (TLR9) ligand CpG induces functional maturation of dendritic cells, the key antigen-presenting cells of the immune system capable of activating tumor-specific CD8$^+$ T cells (36). Therefore, $Ac_5 3F_{ax}Neu5Ac$ treatment was combined with CpG adjuvant injections in the stringent B16-F10^{WT} model (Fig. 7A). CpG injections alone had no significant effect on tumor growth, but the combination of CpG with $Ac_5 3F_{ax}Neu5Ac$ significantly delayed tumor growth and increased the median survival time from 24 days ($Ac_5 3F_{ax}Neu5Ac$ alone) to 35 days (Fig. 7B and C). CpG has been shown to induce dendritic cell maturation in the tumor (36, 37). Accordingly, we found that CpG injections enhanced maturation of CD11c$^+$ dendritic cells in the tumor as shown by the upregulation of the costimulatory molecules CD80 and CD86 (Fig. 7D–F). Interestingly, $Ac_5 3F_{ax}Neu5Ac$ injections alone also increased CD80 and CD86 upregulation, although to lesser extent than CpG. Strikingly, combining both compounds strongly induced dendritic cell maturation in the tumor. This strong upregulation of CD80 and CD86 after combination treatment was also observed in dendritic cells in the tumor-draining lymph node, but not in the non-draining lymph nodes or the spleen (Supplementary Fig. S12). In line with the enhanced dendritic cell maturation in the tumor and tumor-draining lymph node, high numbers of activated CD8$^+$ CD107a$^+$ cytotoxic T cells were detected in tumors after CpG and $Ac_5 3F_{ax}Neu5Ac$ combination treatment (Fig. 7G–J; Supplementary Fig. S13). These data indicate that sialic acid blockade together with the CD8$^+$ T-cell–promoting activity of CpG induces highly potent antitumor immune responses and shows the potential potency of combinatorial strategies with sialic acid blockade.

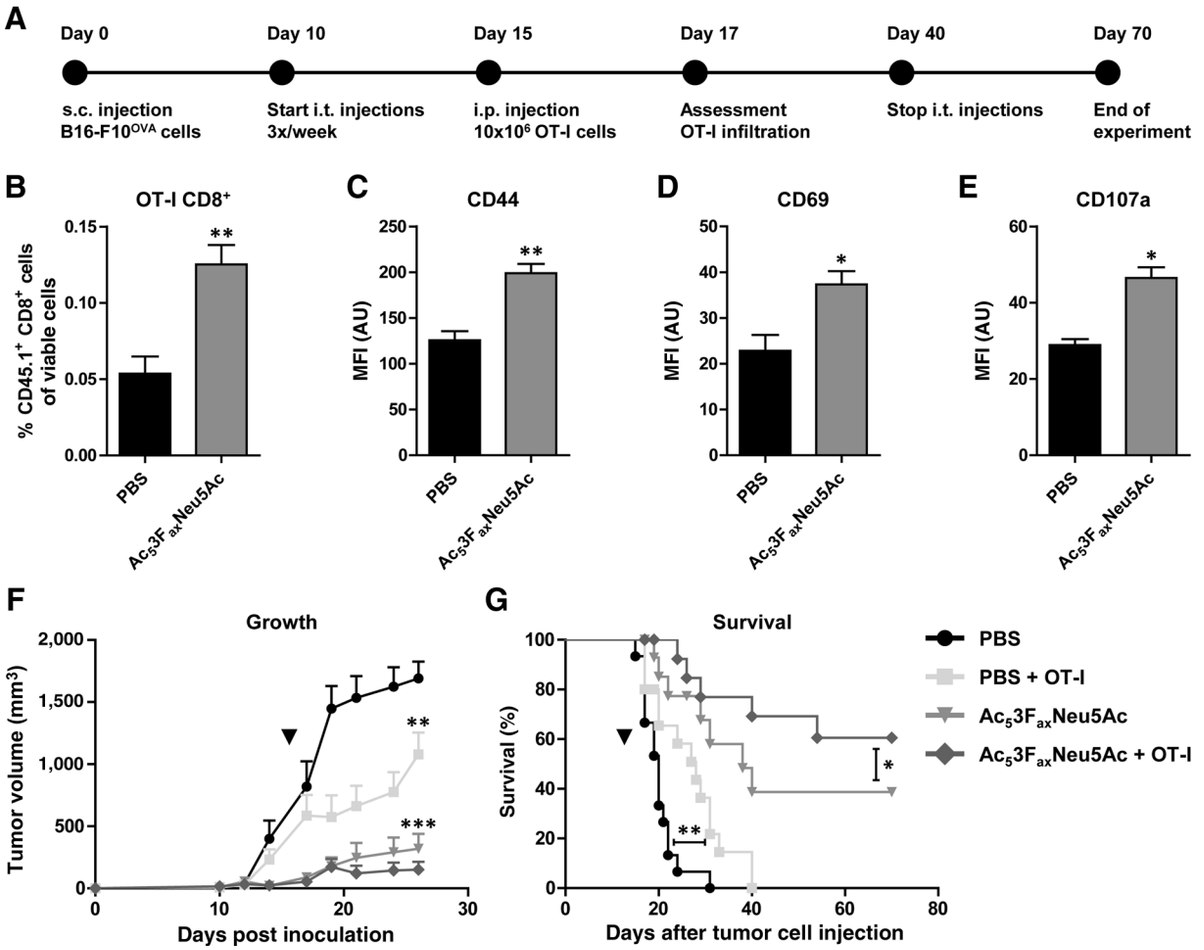

Figure 6.

Intratumoral $Ac_5 3F_{ax}$Neu5Ac injections promote adoptive OT-I $CD8^+$ T-cell transfer therapy. **A–G,** Combined effect of $Ac_5 3F_{ax}$Neu5Ac treatment and adoptive OT-I $CD8^+$ T-cell transfer on B16-$F10^{OVA}$ tumor growth. Schematic representation of the experiment (**A**). Bar diagrams show average percentage ± SEM of tumor-infiltrating $CD45.1^+$ OT-I $CD8^+$ T cells two days after adoptive transfer (**B**) and their expression of activation markers CD44 (**C**), CD69 (**D**), and CD107a (**E**) as average mean fluorescence intensity (MFI) ± SEM ($n = 3$). Graph showing average tumor volume ± SEM (**F**) and Kaplan–Meier curves showing percentage survival (**G**) of the different treatment groups ($n = 12$). Arrow, OT-I $CD8^+$ T-cell transfer. AU, arbitrary unit.

Discussion

Aberrant sialic acid expression has been associated with multiple aspects of tumor growth and progression. Yet, pharmacologic inhibition of sialic acid expression in tumors *in vivo* has not been feasible so far. The therapeutic potential of sialic acid inhibition in cancer therefore remains unexplored. In this study, we investigated the use of the fluorinated sialic acid mimetic $Ac_5 3F_{ax}$Neu5Ac to block sialic acid expression in established tumors and studied its effects on tumor growth, the tumor microenvironment, and tumor immunity. First, we found that repeated intratumoral injections with the sialic acid mimetic were well tolerated and blocked sialic acid expression locally in tumor cells. Sialic acid blockade suppressed B16-$F10^{WT}$ melanoma and 9464D neuroblastoma growth and even had a curative effect in the immunogenic B16-$F10^{OVA}$ tumor model. Second, sialic acid blockade changed the immunosuppressive tumor microenvironment into a more permissive one with higher numbers of activated effector immune cells and significantly less regulatory T cells and myeloid regulatory cells. Third, we found that antitumor effects of $Ac_5 3F_{ax}$Neu5Ac injections were largely mediated by $CD8^+$ effector T cells. Sialic acid blockade rendered tumor cells highly vulnerable to killing by cytotoxic T cells *in vitro* and *in vivo* following adoptive transfer. These data demonstrate that sialic acid blockade enhances the efficacy of cellular immunotherapy. In addition, $Ac_5 3F_{ax}$Neu5Ac injections also potentiated the activation of dendritic cells with CpG *in vivo*. This combination therapy induced a robust $CD8^+$ T-cell response in mice, resulting in strong growth suppression of poorly immunogenic B16-$F10^{WT}$ tumors.

Because of the recent advances in carbohydrate chemistry, glycomimetics like $Ac_5 3F_{ax}$Neu5Ac that can be synthesized in large amounts and with high purity now become available for testing in preclinical models. *In vitro*, $Ac_5 3F_{ax}$Neu5Ac potently blocks sialic acid expression without affecting other glycosylation pathways and even high concentrations and long-term exposure of cancer cells and primary cells with $Ac_5 3F_{ax}$Neu5Ac showed no effect on cell viability or proliferation (24, 26, 38). Accordingly, repeated intratumoral injections with 10 mg/kg sialic acid

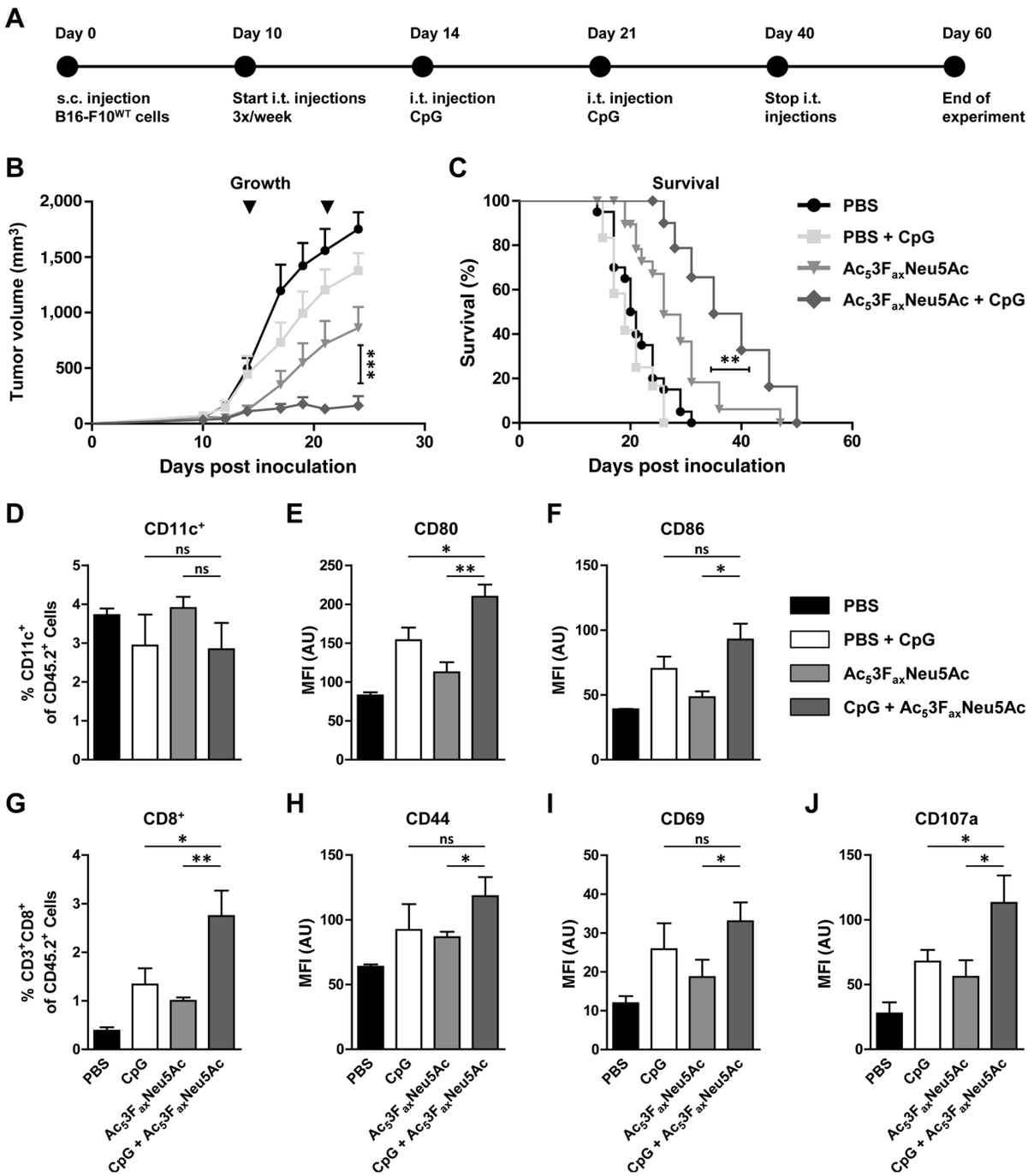

Figure 7.

CpG immune adjuvant increases $Ac_5 3F_{ax}$Neu5Ac -mediated tumor growth suppression. **A,** Schematic representation of the experiment. **B** and **C,** B16-F10^{WT} tumors were injected with PBS or $Ac_5 3F_{ax}$Neu5Ac three times a week, and on day 14 and 21 postinoculation, CpG was coinjected. Graphs show average tumor volume ± SEM (**B**) and survival (**C**) of the different treatment groups. **D–F,** Infiltration and maturation status of CD11c$^+$ dendritic cells. Bar diagrams show mean percentage tumor-infiltrating dendritic cells ± SEM (**D**) and their expression of CD80 (**E**) and CD86 (**F**) as mean fluorescence intensity (MFI) ± SEM ($n = 6$). **G–J,** Number and activation status of CD8$^+$ effector T cells in the tumor after treatment. Mean percentage ± SEM of CD8$^+$ T cells (**G**) as well as their expression of CD44 (**H**), CD69 (**I**), and CD107a is shown (**J**; $n = 6$). AU, arbitrary unit.

mimetic were generally well-tolerated, although prolonged exposure to a higher dose resulted in nephrotoxicity. The intratumoral injections blocked sialic acid expression efficiently in tumor cells, but also a significant reduction in sialic acid expression was found on immune cells. No effect on systemic sialylation was observed after injections with 10 mg/kg $Ac_5 3F_{ax}$Neu5Ac. Probably, due to the intratumoral administration, a large part of the mimetic is retained in the tumor mass, thereby limiting systemic exposure.

Furthermore, our data indicate that B16-F10 cells are more sensitive to sialic acid blockade with $Ac_53F_{ax}Neu5Ac$ compared with the tumor-infiltrating immune cells. Therefore, blocked sialic acid expression in tumor cells is most likely responsible for the observed effects in the tumor microenvironment, although diminished sialic acid expression on the local immune cells may contribute as well. In line with these findings, Wu and colleagues showed that tumor cells have a higher preference to take up sialic acids compared with other tissues (39, 40). We found, however, also a difference in the sensitivity of B16-F10 cells and 9464D cells for $Ac_53F_{ax}Neu5Ac$ *in vitro* and *in vivo*. While 10 mg/kg sialic acid mimetics injections were sufficient to block sialic acid expression in the B16-F10 model, 20 mg/kg were needed to reduce sialic acid expression and tumor growth in the 9464D model. This difference in sensitivity between the two cell types can most likely be explained by differences in uptake of the inhibitor, levels of competing endogenous sialic acid concentrations or sialyltransferase expression levels.

Repeated injections with 10 mg/kg $Ac_53F_{ax}Neu5Ac$ had no effect on systemic sialylation and showed no adverse effects, but injections with a higher dose for several weeks caused a reduction in sialic acid expression in the kidney and resulted in kidney failure and edema formation. Most likely, $Ac_53F_{ax}Neu5Ac$ that is not retained in the tumor can accumulate in the kidney, resulting in reduced sialic acid expression in the glomeruli and disturbed glomerular filtration. These results confirm recent findings by Macauley and colleagues who showed that intravenous administration of 300 mg/kg $Ac_53F_{ax}Neu5Ac$ leads to kidney failure and a study by Galeano and colleagues who showed that a genetic defect in sialic acid synthesis results in defective glomeruli and proteinuria (41, 42). Except for the kidney phenotype, we could not observe any other adverse effects following $Ac_53F_{ax}Neu5Ac$ or $Ac_5Neu5Ac$ injections. Even mice undergoing remission after treatment of the B16-F10^{OVA} tumors with the sialic acid mimetic that were monitored for several months showed no pathologic features. These data strongly suggest that the observed adverse effect on the kidneys is the result of blocked sialic acid expression in the glomeruli, but not related to direct toxic effects of $Ac_53F_{ax}Neu5Ac$. Yet, for the safe use in humans this prototype drug needs to be improved for intratumoral injections or specifically targeted to the tumor cells. Our group has recently encapsulated $Ac_53F_{ax}Neu5Ac$ into tumor-targeting, biodegradable nanoparticles that allowed for the specific delivery of the sialic acid mimetic to melanoma cells in the blood stream (28).

The potent and specific action of $Ac_53F_{ax}Neu5Ac$ enabled us to block sialic acid expression in established tumors. We found that sialic acid blockade had a profound effect on the tumor microenvironment with a strong increase in NK cells, $CD4^+$ and $CD8^+$ T cells and reduced percentages of regulatory T cells as well as myeloid cells. As tumor sialic acids are involved in many processes, it is likely that the impact of sialic acid blockade on the tumor microenvironment is multifactorial (7, 43). Our first mechanistic studies indicate that sialic acid blockade (i) induces proimmune effects including enhanced dendritic cell maturation, and increased numbers and activation state of effector immune cells, especially $CD8^+$ T cells; (ii) decreases immunosuppressive regulatory T cells and myeloid cells in the tumor; (iii) facilitates tumor cell killing by cytotoxic T cells; and (iv) potentiates other cancer immunotherapies. How sialic acid blockade results in these changes in the tumor microenvironment at the molecular level remains to be investigated. Possibly, injections with $Ac_53F_{ax}Neu5Ac$ lead to the loss of tumor sialic acids that can otherwise interact with immune modulatory Siglecs on immune cells. Recently, Beatson and colleagues showed that tumor-derived and heavily sialylated Mucin 1 (MUC1) reprograms myeloid cells in their favor via the interaction with Siglec-9 (16). They showed that MUC1–Siglec-9 interactions stimulated the secretion of tumor-promoting factors (IL6, M-CSF) from myeloid cells. Moreover, MUC1 binding to Siglec-9 induced the differentiation of monocytes to tumor-associated macrophages (TAM). These data strongly support the concept that sialic acid interactions with Siglecs contribute to the formation of the immunosuppressive tumor microenvironment (7, 8, 10, 20–22). In line with these findings, we have observed reduced numbers of myeloid cells in the tumors treated with the glycomimetics. Whether this effect is related to the inhibition of sialic acid–Siglec interactions remains to be investigated. The finding that sialic acid blockade still resulted in a survival benefit in tumor-bearing mice depleted of myeloid cells, emphasizes, however, a role of the inhibitor beyond modulation of myeloid cells. Next to altered Siglec ligand expression, also galectin binding to now uncapped glycans could influence tumor cell growth and progression (44).

While sialic acid blockade can have a broad impact on cancer cells, our data strongly indicate that the increased cell death and growth inhibition, and even complete remission after $Ac_53F_{ax}Neu5Ac$ treatment results from enhanced killing of tumor cells by cytotoxic T cells. This hypothesis is supported by several observations. First, depletion of $CD8^+$ T cells from mice before and after tumor inoculation largely abrogated the antitumor effect of $Ac_53F_{ax}Neu5Ac$ injections. Interestingly, also the depletion of NK cells prior to tumor inoculation abrogated the growth suppression mediated by the glycomimetic, whereas depletion of NK cells after tumor inoculation had no significant effect on $Ac_53F_{ax}Neu5Ac$-mediated growth suppression. These data indicate that NK cells limit B16-F10 take at an early stage after inoculation, but are less relevant for tumor control at a later stage. Second, we detected an increased number of $CD8^+$ T cells present in tumors with sialic acid blockade. These T cells also showed higher expression of the degranulation marker CD107a on their membrane. Third, desialylated B16-F10^{OVA} cells showed an increased susceptibility to killing by OVA-specific $CD8^+$ T cells compared with control cells. Moreover, adoptive transfer of activated $CD8^+$ OT-I T cells further increased tumor rejection in mice treated with $Ac_53F_{ax}Neu5Ac$. It has been suggested that hypersialylation of the Fas receptor protects tumor cells from Fas-mediated killing by cytotoxic T cells and that tumor sialic acids inhibit the release of cytotoxic granules from $CD8^+$ T cells (45, 46). Removal of negatively charged sialic acids could also influence the biophysical interaction between tumor cells and T cells for instance by affecting MHC I–T-cell receptor interactions and subsequent signaling events (43, 47). Accordingly, we observed increased clustering between desialylated B16-F10 and $CD8^+$ OT-I T cells compared with control tumor cells. These findings support the concept that sialic acid blockade advances tumor cell–T-cell interactions. Further research is needed to unravel the mechanisms underlying the enhanced susceptibility of sialic acid–depleted tumor cells to killing by cytotoxic T cells. Enhanced killing by $CD8^+$ T cells, however, is likely to account for the strong tumor rejection observed when combining sialic acid blockade with adoptive T-cell transfer. These findings suggest that the outcome of cellular immunotherapy (e.g. CAR T-cell therapy) could be improved with sialic acid blockade in the tumor cells. It will also be interesting to investigate whether

sialic acid blockade is able to potentiate cancer immunotherapy with immune checkpoint–blocking antibodies like PD-1 and CTLA-4.

Next to promoting adoptive T-cell transfer therapy, we found that sialic acid blockade combined with CpG injections strongly reduced the growth of poorly immunogenic B16-F10^{WT} cells. CpG injected at the tumor site has been shown to functionally mature dendritic cells and to induce robust antitumor CD8$^+$ T-cell responses (36, 37, 48). Indeed, we observed CpG-induced maturation of dendritic cells in the tumor microenvironment and interestingly, sialic acid blockade alone also resulted in increased maturation of dendritic cells. Combined CpG and Ac_53F_{ax}-Neu5Ac coinjections even further enhanced dendritic cell maturation and activated CD8$^+$ T cells numbers in the tumor. Likewise, tumor sialic acids inhibit dendritic cell activation by interacting with immunoinhibitory Siglecs, and therefore suppress the initiation of antitumor immune responses (7, 49, 50). Another explanation could be that Ac_53F_{ax}Neu5Ac has a direct effect on dendritic cells. We recently showed that blocking sialic acid expression in human monocyte-derived dendritic cells with Ac_53F_{ax}Neu5Ac lowered the threshold for activation by TLR ligands, most likely by preventing interactions with immunosuppressive Siglecs (38). These findings thus imply that sialic acid blockade promotes antitumor immunity by facilitating dendritic cell maturation.

We conclude that sialic acid blockade in established tumors is feasible by intratumoral injections of the fluorinated glycomimetic Ac_53F_{ax}Neu5Ac. Such injections significantly reduced melanoma as well as neuroblastoma growth and resulted even in remission in the immunogenic B16-F10^{OVA} model. Sialic acid blockade created an immune permissive tumor microenvironment and rendered tumor cells vulnerable to killing by CD8$^+$ T cells. Sialic acid blockade therefore potentiated the outcome of cellular immunotherapy with CD8$^+$ T cells and strongly favored the induction of antitumor immunity after dendritic cell activation with CpG. These data support the current concept that tumor sialic acids have an immunomodulatory role and participate in tumor immune evasion. Sialic acid blocking glycomimetics such as Ac_53F_{ax}Neu5Ac could therefore help to overcome the immune suppressive tumor microenvironment to permit strong tumor immune responses, alone or in combination with existing immunotherapies.

Disclosure of Potential Conflicts of Interest

No potential conflicts of interest were disclosed.

Authors' Contributions

Conception and design: C. Büll, T.J. Boltje, M.H. den Brok, G.J. Adema
Development of methodology: C. Büll, M. Wassink, T. Heise, M.H. den Brok, G.J. Adema
Acquisition of data (provided animals, acquired and managed patients, provided facilities, etc.): C. Büll, N. Balneger, S.M. Weischer, M. Wassink, J.J. van Gemst, L. Boon, J. van der Vlag
Analysis and interpretation of data (e.g., statistical analysis, biostatistics, computational analysis): C. Büll, N. Balneger, S.M. Weischer, J.J. van Gemst, J. van der Vlag, G.J. Adema
Writing, review, and/or revision of the manuscript: C. Büll, T.J. Boltje, N. Balneger, L. Boon, M.H. den Brok, G.J. Adema
Administrative, technical, or material support (i.e., reporting or organizing data, constructing databases): C. Büll, M. Wassink, T. Heise
Study supervision: T.J. Boltje, M.H. den Brok, G.J. Adema
Other (synthetic probe synthesis): V.R.L.J. Bloemendal
Other (synthesis of chemicals): T. Heise

Acknowledgments

This work was supported by a Radboudumc grant (awarded to C. Büll), a VENI grant from the Netherlands Organization for Scientific Research (NWO; awarded to T.J. Boltje), a Marie Skøodowska-Curie Innovative Training Network (ITN-ETN 641549; awarded to G.J. Adema), and KWF grants [awarded to G.J. Adema and M.H. den Brok (KWF20136-6111), G.J. Adema (KWF11266), and G.J. Adema, T.J. Boltje, and C. Büll (KUN2015-7604)].

The costs of publication of this article were defrayed in part by the payment of page charges. This article must therefore be hereby marked *advertisement* in accordance with 18 U.S.C. Section 1734 solely to indicate this fact.

Received November 1, 2017; revised March 14, 2018; accepted April 16, 2018; published first April 27, 2018.

References

1. Pinho SS, Reis CA. Glycosylation in cancer: mechanisms and clinical implications. Nat Rev Cancer 2015;15:540–55.
2. Varki A, Schnaar RL, Schauer R. Sialic acids and other nonulosonic acids. In: Varki A, Cummings RD, Esko JD, Stanley P, Hart GW, Aebi M, et al. , editors. Essentials of glycobiology. Cold Spring Harbor, NY: Cold Spring Harbor Laboratory Press; 2015. p 179–95.
3. Büll C, Stoel MA, den Brok MH, Adema GJ. Sialic Acids Sweeten a Tumor's Life. Cancer Res 2014;74:3199–204.
4. Fuster MM, Esko JD. The sweet and sour of cancer: glycans as novel therapeutic targets. Nat Rev Cancer 2005;5:526–42.
5. Astronomo RD, Burton DR. Carbohydrate vaccines: developing sweet solutions to sticky situations? Nat Rev Drug Discov 2010;9:308–24.
6. Heimburg-Molinaro J, Lum M, Vijay G, Jain MT, Almogren A, Rittenhouse-Olson K. Cancer vaccines and carbohydrate epitopes. Vaccine 2011;29: 8802–26.
7. Büll C, den Brok MH, Adema GJ. Sweet escape: sialic acids in tumor immune evasion. Biochim Biophys Acta 2014;1846:238–46.
8. Pearce OM, Laubli H. Sialic acids in cancer biology and immunity. Glycobiology 2016;26:111–28.
9. Cohen M, Elkabets M, Perlmutter M, Porgador A, Voronov E, Apte RN, et al. Sialylation of 3-Methylcholanthrene-Induced Fibrosarcoma Determines Antitumor Immune Responses during Immunoediting. J Immunol 2010;185:5869–78.
10. Boligan KF, Mesa C, Fernandez LE, von Gunten S. Cancer intelligence acquired (CIA): tumor glycosylation and sialylation codes dismantling antitumor defense. Cell Mol Life Sci 2015;72:1231–48.
11. Sedlacek HH, Seiler FR. Immunotherapy of neoplastic diseases with neuraminidase - contradictions, new aspects, and revised concepts. Cancer Immunol Immunother 1978;5:153–63.
12. Sanford BH. An alteration in tumor histocompatibility induced by neuraminidase. Transplantation 1967;5:1273–9.
13. Bagshawe KD, Currie GA. Immunogenicity of L 1210 murine leukaemia cells after treatment with neuraminidase. Nature 1968;218:1254–5.
14. Jandus C, Boligan KF, Chijioke O, Liu H, Dahlhaus M, Demoulins T, et al. Interactions between Siglec-7/9 receptors and ligands influence NK cell-dependent tumor immunosurveillance. J Clin Invest 2014;124:1810–20.
15. Hudak JE, Canham SM, Bertozzi CR. Glycocalyx engineering reveals a Siglec-based mechanism for NK cell immunoevasion. Nat Chem Biol 2014;10:69–U111.
16. Beatson R, Tajadura-Ortega V, Achkova D, Picco G, Tsourouktsoglou TD, Klausing S, et al. The mucin MUC1 modulates the tumor immunological microenvironment through engagement of the lectin Siglec-9. Nat Immunol 2016;17:1273–81.
17. Büll C, Heise T, van Hilten N, Pijnenborg JF, Bloemendal VR, Gerrits L, et al. Steering siglec-sialic acid interactions on living cells using bioorthogonal chemistry. Angew Chem 2017;56:3309–13.

18. Xiao H, Woods EC, Vukojicic P, Bertozzi CR. Precision glycocalyx editing as a strategy for cancer immunotherapy. Proc Natl Acad Sci U S A 2016; 113:10304–9.
19. Läubli H, Pearce OM, Schwarz F, Siddiqui SS, Deng L, Stanczak MA, et al. Engagement of myelomonocytic Siglecs by tumor-associated ligands modulates the innate immune response to cancer. Proc Natl Acad Sci U S A 2014;111:14211–6.
20. Muenst S, Laubli H, Soysal SD, Zippelius A, Tzankov A, Hoeller S. The immune system and cancer evasion strategies: therapeutic concepts. J Intern Med 2016;279:541–62.
21. Fraschilla I, Pillai S. Viewing Siglecs through the lens of tumor immunology. Immunol Rev 2017;276:178–91.
22. Adams OJ, Stanczak MA, von Gunten S, Laubli H. Targeting sialic acid-Siglec interactions to reverse immune suppression in cancer. Glycobiology. 2017 Dec 22. [Epub ahead of print].
23. Perdicchio M, Cornelissen LA, Streng-Ouwehand I, Engels S, Verstege MI, Boon L, et al. Tumor sialylation impedes T cell mediated anti-tumor responses while promoting tumor associated-regulatory T cells. Oncotarget 2016;7:8771–82.
24. Rillahan CD, Antonopoulos A, Lefort CT, Sonon R, Azadi P, Ley K, et al. Global metabolic inhibitors of sialyl- and fucosyltransferases remodel the glycome. Nat Chem Biol 2012;8:661–8.
25. Büll C, Heise T, Beurskens DM, Riemersma M, Ashikov A, Rutjes FP, et al. Sialic acid glycoengineering using an unnatural sialic acid for the detection of sialoglycan biosynthesis defects and on-cell synthesis of siglec ligands. ACS Chem Biol 2015;10:2353–63.
26. Büll C, Boltje TJ, Wassink M, de Graaf AM, van Delft FL, den Brok MH, et al. Targeting aberrant sialylation in cancer cells using a fluorinated sialic acid analog impairs adhesion, migration, and in vivo tumor growth. Mol Cancer Ther 2013;12:1935–46.
27. Burkart MD, Vincent SP, Wong CH. An efficient synthesis of CMP-3-fluoroneuraminic acid. Chem Commun 1999:1525–6.
28. Büll C, Boltje TJ, van Dinther EA, Peters T, de Graaf AM, Leusen JH, et al. Targeted delivery of a sialic acid-blocking glycomimetic to cancer cells inhibits metastatic spread. ACS Nano 2015;9:733–45.
29. Falo LD, Kovacsovicsbankowski M, Thompson K, Rock KL. Targeting antigen into the phagocytic pathway in-vivo induces protective tumor-immunity. Nat Med 1995;1:649–53.
30. Kroesen M, Nierkens S, Ansems M, Wassink M, Orentas RJ, Boon L, et al. A transplantable TH-MYCN transgenic tumor model in C57Bl/6 mice for preclinical immunological studies in neuroblastoma. Int J Cancer 2014;134:1335–45.
31. Stauffer JK, Orentas RJ, Lincoln E, Khan T, Salcedo R, Hixon JA, et al. High-throughput molecular and histopathologic profiling of tumor tissue in a novel transplantable model of murine neuroblastoma: new tools for pediatric drug discovery. Cancer Invest 2012;30:343–63.
32. Garsen M, Benner M, Dijkman HB, van Kuppevelt TH, Lo JP, RabeLink TJ, et al. Heparanase is essential for the development of acute experimental glomerulonephritis. Am J Pathol 2016;186:805–15.
33. Rops AL, Gotte M, Baselmans MH, van den Hoven MJ, Steenbergen EJ, Lensen JF, et al. Syndecan-1 deficiency aggravates anti-glomerular basement membrane nephritis. Kidney Int 2007;72:1204–15.
34. Hurez V, Daniel BJ, Sun L, Liu AJ, Ludwig SM, Kious MJ, et al. Mitigating age-related immune dysfunction heightens the efficacy of tumor immunotherapy in aged mice. Cancer Res 2012;72:2089–99.
35. Chen D, Xie J, Fiskesund R, Dong W, Liang X, Lv J, et al. Chloroquine modulates antitumor immune response by resetting tumor-associated macrophages toward M1 phenotype. Nat Commun 2018;9:873.
36. Klinman DM. Immunotherapeutic uses of CpG oligodeoxynucleotides. Nat Rev Immunol 2004;4:249–58.
37. den Brok MHMGM, Sutmuller RPM, Nierkens S, Bennink EJ, Toonen LWJ, Figdor CG, et al. Synergy between in situ cryoablation and TLR9 stimulation results in a highly effective in vivo dendritic cell vaccine. Cancer Res 2006;66:7285–92.
38. Büll C, Collado-Camps E, Kers-Rebel ED, Heise T, Sondergaard JN, den Brok MH, et al. Metabolic sialic acid blockade lowers the activation threshold of moDCs for TLR stimulation. Immunol Cell Biol 2017;95: 408–15.
39. Wu XJ, Tian YP, Yu MZ, Lin BJ, Han JH, Han SF. A fluorescently labelled sialic acid for high performance intraoperative tumor detection. Biomater Sci 2014;2:1120–7.
40. Wu XJ, Yu MZ, Lin BJ, Xing HJ, Han JH, Han SF. A sialic acid-targeted near-infrared theranostic for signal activation based intraoperative tumor ablation. Chem Sci 2015;6:798–803.
41. Macauley MS, Arlian BM, Rillahan CD, Pang PC, Bortell N, Marcondes MC, et al. Systemic blockade of sialylation in mice with a global inhibitor of sialyltransferases. J Biol Chem 2014;289:35149–58.
42. Galeano B, Klootwijk R, Manoli I, Sun M, Ciccone C, Darvish D, et al. Mutation in the key enzyme of sialic acid biosynthesis causes severe glomerular proteinuria and is rescued by N-acetylmannosamine. J Clin Invest 2007;117:1585–94.
43. Varki A, Gagneux P. Multifarious roles of sialic acids in immunity. Ann Ny Acad Sci 2012;1253:16–36.
44. Zhuo Y, Bellis SL. Emerging role of alpha2,6-sialic acid as a negative regulator of galectin binding and function. J Biol Chem 2011;286: 5935–41.
45. Swindall AF, Bellis SL. Sialylation of the Fas death receptor by ST6Gal-I provides protection against Fas-mediated apoptosis in colon carcinoma cells. J Biol Chem 2011;286:22982–90.
46. Lee HC, Wondimu A, Liu YH, Ma JSY, Radoja S, Ladisch S. Ganglioside inhibition of CD8(+) T cell cytotoxicity: interference with lytic granule trafficking and exocytosis. J Immunol 2012;189:3521–7.
47. Daniels MA, Levine L, Miller JD, Moser JM, Lukacher AE, Altman JD, et al. CD8 binding to MHC class I molecules is influenced by maturation and T cell glycosylation. Immunity 2001;15:1051–61.
48. Krieg AM. Development of TLR9 agonists for cancer therapy. J Clin Invest 2007;117:1184–94.
49. Ohta M, Ishida A, Toda M, Akita K, Inoue M, Yamashita K, et al. Immunomodulation of monocyte-derived dendritic cells through ligation of tumor-produced mucins to Siglec-9. Biochem Biophys Res Commun 2010;402:663–9.
50. Ding Y, Guo Z, Liu Y, Li X, Zhang Q, Xu X, et al. The lectin Siglec-G inhibits dendritic cell cross-presentation by impairing MHC class I-peptide complex formation. Nat Immunol 2016;17:1167–75.